nature food

Article

https://doi.org/10.1038/s43016-023-00848-0

Root microbiota confers rice resistance to aluminium toxicity and phosphorus deficiency in acidic soils

Received: 9 January 2023

Accepted: 5 September 2023

Published online: 2 October 2023

Check for updates

Chaoyang Liu[1,8], Meitong Jiang[1,2,8], Mengting Maggie Yuan[3,8], Ertao Wang[4], Yang Bai[5], Thomas W. Crowther[6], Jizhong Zhou[7], Zhiyuan Ma[1], Li Zhang[1,2], Yu Wang[1], Jixian Ding[1], Wuxing Liu[1], Bo Sun[1], Renfang Shen[1], Jiabao Zhang[1] & Yuting Liang[1]

Aluminium (Al) toxicity impedes crop growth in acidic soils and is considered the second largest abiotic stress after drought for crops worldwide. Despite remarkable progress in understanding Al resistance in plants, it is still unknown whether and how the soil microbiota confers Al resistance to crops. Here we found that a synthetic community composed of highly Al-resistant bacterial strains isolated from the rice rhizosphere increased rice yield by 26.36% in acidic fields. The synthetic community harvested rhizodeposited carbon for successful proliferation and mitigated soil acidification and Al toxicity through extracellular protonation. The functional coordination between plants and microbes offers a promising way to increase the usage of legacy phosphorus in topsoil. These findings highlight the potential of microbial tools for advancing sustainable agriculture in acidic soils.

Acidic soils compose 40–50% of the world's potentially arable lands[1]. Acidic soils with pH <5.5 account for 39.5 million hm^2 of land globally. Crops grown in these soils are often prone to aluminium (Al) toxicity stress, which is considered the second largest abiotic stress for crops after drought[2,3]. The rhizotoxic Al^{3+} solubilized in acidic soils can cause substantial damage to plant roots, inhibit root elongation by 40% and lead to a short-stunted root system[4]. Within the roots, Al depresses cell division, cell elongation and membrane polarization while it also reduces photosynthetic efficiency and pigments in leaves[5]. It also causes overaccumulation of reactive oxygen species that can inordinate cell wall proteins and other metabolic pathways[6]. As a result, crops intoxicated by Al suffer from accompanying mineral nutrient deficiencies, hindering crop performance[7].

Approximately 13% (3.25 million hm^2) of the world's rice (*Oryza sativa* L.) is grown in acidic soils, mainly distributed in tropical and subtropical regions[2]. The physiological, genetic and molecular mechanisms of rice resistance to Al toxicity have been studied extensively, as Al resistance-associated genes provide potential engineering targets for breeding high-yield varieties of plants in acidic soils[8,9]. However, the substantial benefits of plant–microbe interactions in acidic soils remain overlooked, which may open up new opportunities to sustainably increase crop Al resistance and productivity[10].

[1]State Key Laboratory of Soil and Sustainable Agriculture, Institute of Soil Science, Chinese Academy of Sciences, Nanjing, China. [2]University of Chinese Academy of Sciences, Beijing, China. [3]Department of Environmental Science Policy and Management, University of California, Berkeley, CA, USA. [4]National Key Laboratory of Plant Molecular Genetics, CAS Center for Excellence in Molecular Plant Sciences, Institute of Plant Physiology and Ecology, SIBS, Chinese Academy of Sciences, Shanghai, China. [5]State Key Laboratory of Plant Genomics, Institute of Genetics and Developmental Biology, Chinese Academy of Sciences, Beijing, China. [6]Department of Environmental Systems Science, Institute of Integrative Biology, ETH Zurich, Zurich, Switzerland. [7]Department of Microbiology and Plant Biology, University of Oklahoma, Norman, OK, USA. [8]These authors contributed equally: Chaoyang Liu, Meitong Jiang, Mengting Maggie Yuan. e-mail: ytliang@issas.ac.cn

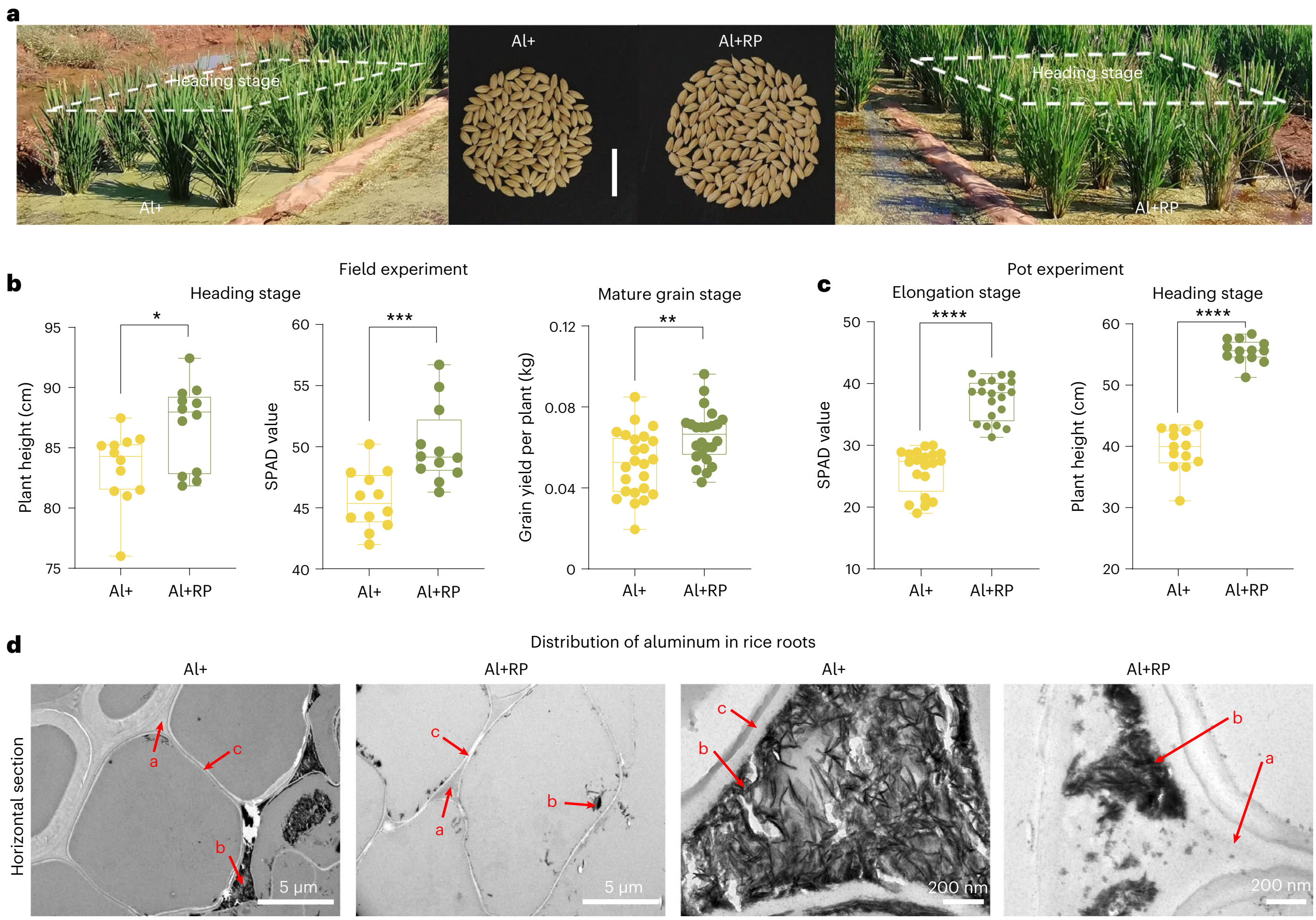

Fig. 1 | SynCom promotes rice performance under Al-toxic acidic stress. **a**–**c**, Nanjing 46 rice plant phenotype and grain yield in the field (**a**, **b**) and pot experiments (**c**) at different growth stages. Scale bar in **a** is 2 cm. In the field experiment (**b**), the plant heights and soil plant analysis development (SPAD) values of three healthy rice plants were measured, and the grain yields of six rice plants were weighed in each plot. Each box in box plot aggregates data points from $n = 4$ biological replicate field plots for each treatment. The two-sided unpaired t-test was used for statistical significance testing (plant height, $P = 0.0174$; SPAD value, $P = 0.0008$; Grain yield per plant, $P = 0.0021$). $^{*}P < 0.05$, $^{**}P < 0.01$, $^{***}P < 0.001$. In the pot experiment (**c**), $n = 20$ biological replicates of rice plants were evaluated for SPAD value, and $n = 13$ biological replicates of rice plants were measured for plant height. The two-sided unpaired t-test method was used for statistical significance testing (SPAD value, $^{****}P < 0.0001$; plant height, $^{****}P < 0.0001$). In **b** and **c**, the horizontal bars represent medians. The tops and bottoms of the boxes show the 75th and 25th percentiles, respectively. The whiskers extend to minimum and maximum value. **d**, Distribution of Al in rice roots was observed by transmission electron microscopy. The red 'a' represents intercellular substances, the red 'b' represents Al and the red 'c' represents the cell wall.

The rhizosphere microbiome provides important support for crop stress tolerance and growth[10]. Plant growth-promoting rhizobacteria (PGPR) provide a range of essential biological functions, such as improving plant nutrient acquisition, pathogen tolerance and stress tolerance[11,12]. Numerous studies have investigated PGPR involvement in conferring plant tolerance to heavy metals (for example, cadmium, copper and manganese) by changing the metal bioavailability through releasing organic acids and siderophores[13,14]. Synthetic communities (SynComs) are assemblies of individual microbial cultures with plant beneficial traits[15]. They have been shown to benefit plants via bottom-up control of nutrient acquisition or pathogen suppression in gnotobiotic systems[16,17]. PGPRs with desired functional traits can be used in SynComs to promote host growth and health under stressed conditions[18,19]. The discovery of a few Al-tolerant PGPRs, including *Paenibacillus yonginensis* DCY84 and *Rhodotorula mucilaginosa* CAM4 (refs. 20,21), inspired our exploration of potential ways to increase rice yield under acid and Al stress through microbial strategies. Can these Al-tolerant microbes reduce Al toxicity while promoting rice growth? What are possible mechanisms involved? Answers to these questions are the first steps to designing a functional SynCom offering persistent protection against Al stress for plants.

In this Article, given the considerable damage to the root system and the accompanying P deficiency caused by Al toxicity in acidic soil, we hypothesized that assembling and applying a proper Al-resistant SynCom could improve rice Al resistance by optimizing root morphology and improving soil nutrient availability. Our aims are (1) to identify Al-resistant bacteria and develop an efficient Al-resistant SynCom, (2) to evaluate the effectiveness of SynCom in promoting rice growth and (3) to elucidate the potential mechanisms of SynCom in conferring rice Al resistance and P uptake. Our study provides a crosstalk-based solution to underpin crop yield improvement and agricultural sustainability through plant–soil–microbiome interactions in widely distributed acidic soils.

Results

Al-resistance evaluation and development of the SynCom

To identify Al-resistant bacteria and develop an efficient Al-resistant SynCom, we established a library of 248 bacterial strains from 421

https://doi.org/10.1038/s43016-023-00848-0

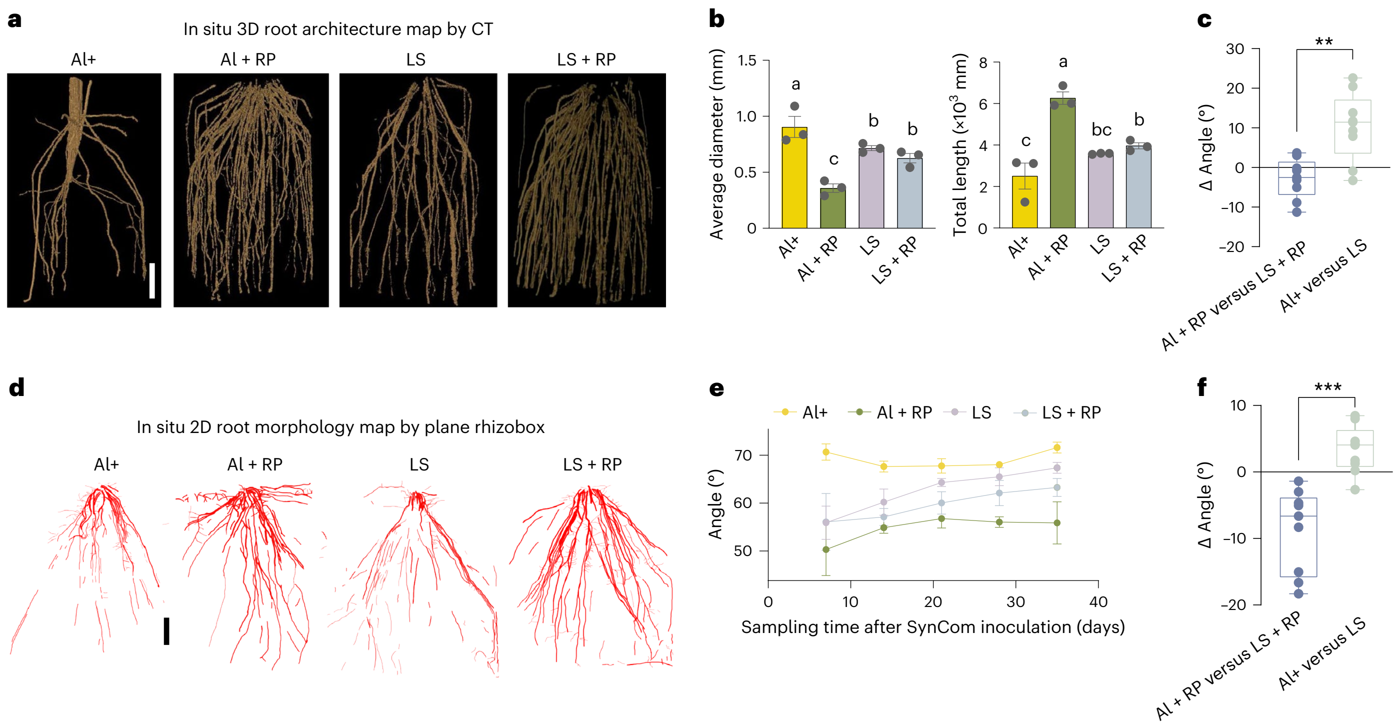

Fig. 2 | Effects of SynCom inoculation on rice root architecture under different treatment conditions. **a**, In situ 3D rice root architecture of Nanjing 46 beneath the soil is non-destructively visualized by X-ray CT technology. See Supplementary Videos 1, 2, 3 and 4. Scale bar, 1 cm. **b**,**c**, Differences in root diameter, total length and root angle by CT images. **d**, In situ 2D rice root architecture of Nanjing 46 by rhizobox methods and root drawing. The red lines indicate traced roots from the images. Scale bar, 2 cm. **e**, Temporal dynamics of the root angle of Nanjing 46 in the rhizobox. **f**, Differences in root angle of Nanjing 46. In **b**–**f**, $n = 3$ biological replicates. In **b** and **e**, data are presented as mean ± s.e.m. The different letters in **b** indicate significant differences ($P < 0.05$, one-way analysis of variance, Fisher's least significant difference test). For P values, see source data. In **c** and **f**, the horizontal bars in box plots represent medians. The tops and bottoms of the boxes show the 75th and 25th percentiles, respectively. The whiskers extend to minimum and maximum value. The two-sided unpaired t-test was used for statistical significance testing in **c** ($P = 0.0011$) and **f** ($P = 0.0001$). $^{**}P < 0.01$, $^{***}P < 0.001$.

isolates obtained from the rhizosphere of *japonica* Nanjing 46 grown in an acidic field (Supplementary Fig. 1 and Supplementary Table 1). The rhizosphere soil pH was approximately 4.86 with an Al^{3+} content of 0.62 mg l^{-1}. These species were probably evolutionarily beneficial to rice in acidic Al-toxic soils and could be SynCom candidates. According to their relative abundance in the rhizosphere and phylogenetic relationships at the genus level, we evaluated 12 representative strains in the library for their Al resistance levels at pH 4.0 on the basis of Raman-D_2O spectroscopy, including two strains each of *Paenibacillus*, *Lysinibacillus* and *Burkholderia*, three strains of *Bacillus*, and one strain each of *Leucobacter*, *Pseudomonas* and *Rhodococcus* (Supplementary Fig. 2 and Supplementary Text 2.1). The C–D ratios indicated that *Pseudomonas* sp. (D95) and *Rhodococcus* sp. (D96) showed the highest Al resistance compared with the other ten strains under 5 mM Al^{3+} added conditions. The concentration dependence–growth curves (0–1.0 mM Al^{3+}, pH 4.0) confirmed that *Pseudomonas* sp. and *Rhodococcus* sp. were Al-resistant strains (Supplementary Fig. 3 and Supplementary Table 2). They were further identified as *R. erythropolis* and *P. aeruginosa* on the basis of full-length 16S ribosomal RNA (rRNA) gene sequence homology. The relative abundances of *R. erythropolis* and *P. aeruginosa* in the rhizosphere from which they were isolated were 0.032% and 0.013%, respectively.

Although laboratory studies have reported the metabolic versatility and plant beneficial traits of *R. erythropolis* and *P. aeruginosa* isolates[22,23], their Al tolerance or ability to protect plants against Al stress remains unknown. Using pot experiments, we found that single inoculation of *R. erythropolis* and *P. aeruginosa* promoted rice shoot and root biomass by 73.8–74.9% and 78.7–108.2%, respectively, while co-inoculation resulted in a 297.4–308.1% increase in rice plant biomass compared with that without inoculation (Supplementary Fig. 4). Hence, the co-culture of *R. erythropolis* and *P. aeruginosa* was constructed as an Al-resistant SynCom, hereafter referred to as RP.

SynCom promoted rice growth and alleviated Al toxicity

We investigated the effects of SynCom on rice performance and grain yield in acidic Al stress soils (Al+, Al + RP) under both field and greenhouse conditions. In the acidic field, SynCom inoculation significantly increased plant height and leaf chlorophyll content by 4.15% and 9.81%, respectively, during the growth stage, as well as grain yield by 26.36% at maturity (Al + RP versus Al+) (Fig. 1a,b). Pot experiments confirmed the promotion effects (Fig. 1c and Supplementary Fig. 5a). We then confirmed in the pot experiment using 16S rRNA quantitative polymerase chain reaction (qPCR) that both *R. erythropolis* and *P. aeruginosa* stably colonized the rice rhizosphere, thriving at the elongation and heading stages (Supplementary Figs. 5b and 6).

Additionally, since heavy metals, such as Al, would cause an overaccumulation of reactive oxygen species that could be scavenged by peroxidase[6], we found that the peroxidase activity was significantly promoted by 128.3% with SynCom in the root tissue (Al + RP versus Al+) (Supplementary Fig. 7a). Transmission electron microscopy combined with energy-dispersive X-ray spectroscopy showed a reduced Al content in root tissue (Fig. 1d, Supplementary Fig. 7b). We further quantified the Al content in root tissue collected from the pot experiment and found that the Al content decreased by 26.5% with SynCom inoculation (Supplementary Fig. 7c).

Liming is a comprehensive measure that improves physicochemical properties for acidic soils (for example, pH, metal and mineral nutrient bioavailability)[24]. Accordingly, we compared the effects of SynCom

https://doi.org/10.1038/s43016-023-00848-0

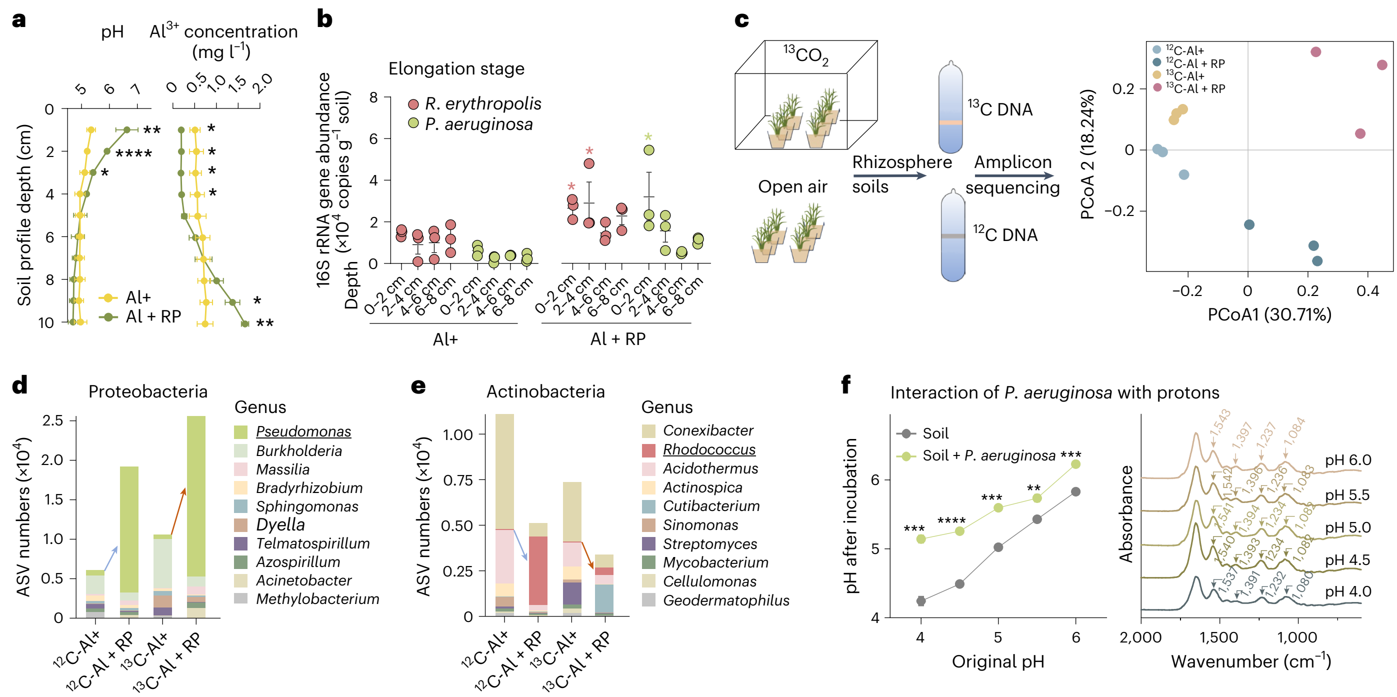

Fig. 3 | Variation in soil chemical properties and bacterial communities after SynCom inoculation. **a**, pH and Al^{3+} concentrations at different soil profile depths. **b**, Colonization of SynCom was determined by qPCR. Red and green asterisks indicate a significantly higher abundance in Al + RP than in Al+ at the same soil depth. **c**–**e**, Determination of the effect of SynCom on bacterial communities by ^{13}C-DNA-SIP. In **c**, shows difference in microbial community structure. In **d**, shows community composition of Proteobacteria. In **e**, shows community composition of Actinobacteria. $n = 3$ biological replicates. The blue and red arrows in **d** and **e** indicate that the abundance of *Pseudomonas* and *Rhodococcus* increased in ^{12}C-Al + RP compared with ^{12}C-Al+ and in ^{13}C-Al + RP compared with ^{13}C-Al+, respectively. The underline in **d** and **e** indicates the genus to which SynCom belongs. **f**, Interaction of *P. aeruginosa* with protons at various pH values. Left: inoculation of *P. aeruginosa* increased the original pH. Right: attenuated total reflectance-Fourier transform infra-red spectra of *P. aeruginosa* at various pH values. In **a**, **b** and **f**, data are presented as mean ± s.e.m. of three biological replicates. The two-sided unpaired *t*-test was used for statistical significance testing. In **a**, pH, $P = 0.0065$, $P < 0.0001$, $P = 0.0464$; Al^{3+} concentration, $P = 0.0201$, $P = 0.0391$, $P = 0.0255$, $P = 0.0339$, $P = 0.0184$, $P = 0.0014$. In **b**, *R. erythropolis*, $P = 0.0182$, $P = 0.0299$; *P. aeruginosa*, $P = 0.0277$. In **c**, $P = 0.0004$, $P < 0.0001$, $P = 0.0003$, $P = 0.0043$, $P = 0.0003$. $^{*}P < 0.05$, $^{**}P < 0.01$, $^{****}P < 0.0001$.

inoculation with traditional lime application on acid stress mitigation. We used $CaCO_3$ to raise the soil pH to above 5.5 and precipitate Al^{3+} (hereafter limed soil, LS and LS + RP). The experiments on four rice varieties (*japonica* Nanjing46 and Nipponbare, *indica* Shanhanzinuo and Jinguoyin) showed that SynCom promoted the chlorophyll content, biomass and root:shoot ratio by 10.3–155.8%, 525.4% and 16.3%, respectively, under Al stress (Al + RP versus Al+) and by 6.94–82.9%, 228.7% and 22.0%, respectively, under limed soil conditions (LS + RP versus LS) (Supplementary Figs. 8 and 9, and Supplementary Text 2.2). Furthermore, rice exhibited better growth with SynCom inoculation under Al stress than limed soil, with the chlorophyll content increasing by 0.06–23.3% and biomass increasing by 8.77% (Al + RP versus LS + RP). To validate the findings with a more defined control over the chemical interactions of different nutrients, we conducted a plant growth promotion assay in a clay-based system without soil matrixes (Supplementary Fig. 10a,b). We found that the promotion effect of SynCom was better under low P (0.5 mg l^{-1}) than under high P (6 mg l^{-1}) at 0 mM Al^{3+} and pH 4.0 (Supplementary Fig. 10c). With increasing Al concentration at pH 4.0, SynCom promoted rice growth better at low P and medium P levels (2.5 mg l^{-1}). The results indicated that SynCom may serve as a more effective way to improve crop growth in acidic soil than traditional lime application.

Optimization of root architecture

Considering that Al toxicity directly inhibits root elongation, resulting in a short, stunted root system, we further examined whether rice growth and yield enhancement with SynCom could be attributed to root development. First, we scanned the root morphology of the four rice varieties (Supplementary Fig. 11). SynCom promoted root growth regardless of the presence of Al stress (Supplementary Fig. 12a,b). More importantly, in Al + RP versus LS + RP, the root length and tips increased by 0.45–75.3% and 5.48–50.00%, respectively, while the average diameter and volume of roots decreased by 14.1–44.5% and 25.6–44.5%, respectively, across the four rice varieties (Supplementary Figs. 12c and 13). This suggested that SynCom promoted the development of fine roots and root hairs in acidic soils, which represents a resource acquisition strategy for plants in nutrient-deficient environments.

We further visualized the three-dimensional (3D) in situ root architecture using CT scanning (Fig. 2a and Supplementary Videos 1, 2, 3 and 4). The results confirmed that the root length was the longest and the root diameter was the smallest in the Al + RP treatment compared with the other treatments (Fig. 2b). The root growth angle was obtained by in situ root architecture analysis, which determines the direction of root elongation. SynCom decreased root angle in Al + RP versus Al+ and LS + RP versus LS by 11.6° and 1.7°, respectively (Supplementary Fig. 14a). Interestingly, the root angle decreased by 2.78° on average with SynCom inoculation in Al + RP versus LS + RP, indicating that more roots grew towards the soil surface (Fig. 2c).

To verify the variation in root angle, we designed a plane rhizobox allowing the full growth and extension of the root system (Supplementary Fig. 15). The root angle was visualized by in situ photography and root drawing (Fig. 2d). Consistent with CT scanning, the results from the rhizobox further demonstrated that rice roots developed towards the shallow root type by SynCom (Fig. 2e,f and Supplementary Fig. 14b).

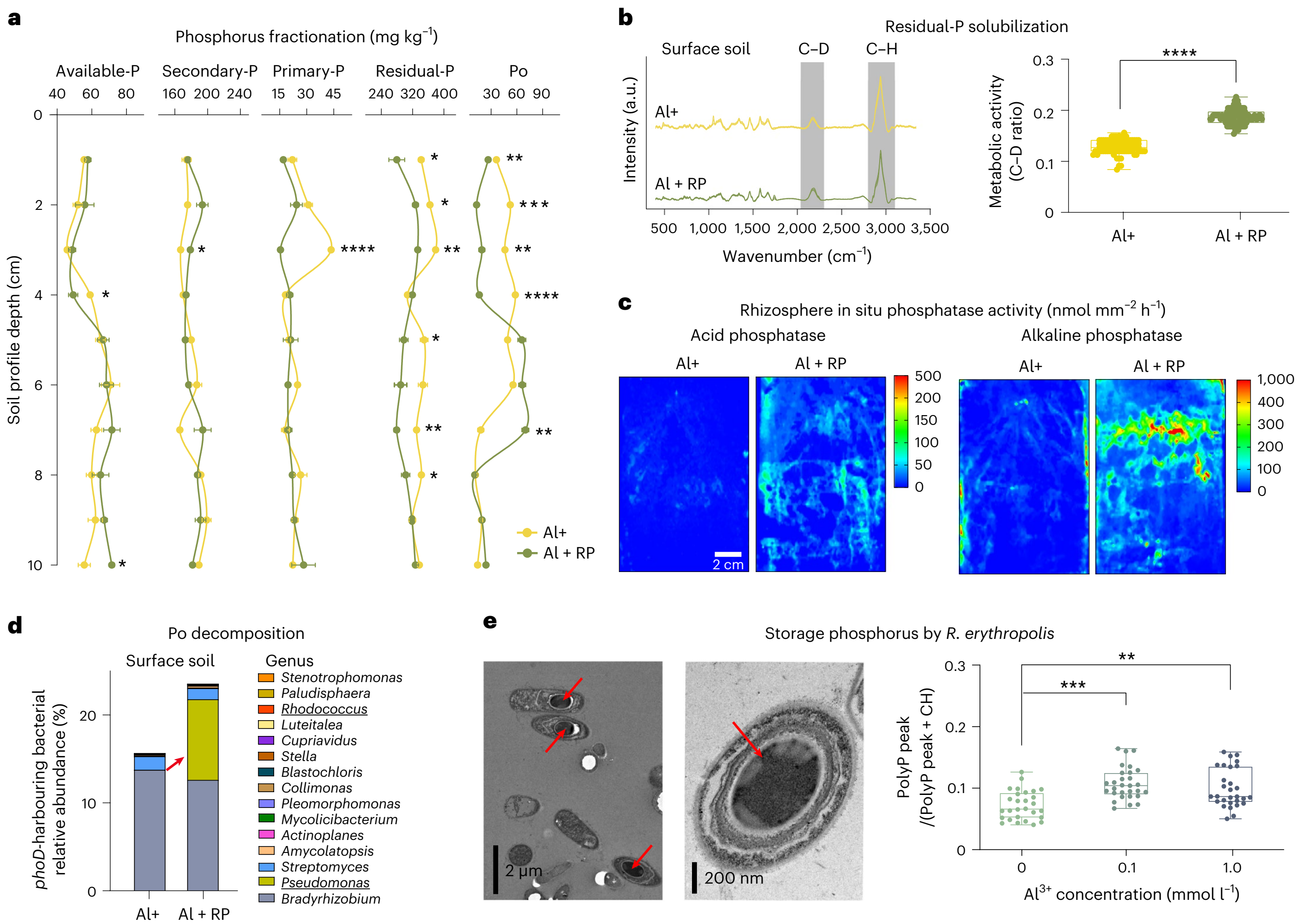

Fig. 4 | The colonization of SynCom assists rice in obtaining surface soil phosphorous under Al-toxic acidic stress. a, Different forms and fractions of phosphorous at different soil profile depths. Po represents organic phosphorous. Data are presented as mean ± s.e.m. of three biological replicates. The two-sided unpaired *t*-test method was used for statistical significance testing (available-P, $P = 0.0113$, $P = 0.0275$; secondary-P, $P = 0.0458$; primary-P, $P < 0.0001$; residual-P, $P = 0.0382$, $P = 0.0226$, $P = 0.0039$, $P = 0.0458$, $P = 0.0051$, $P = 0.0456$; Po, $P = 0.0042$, $P = 0.0004$, $P = 0.0037$, $P < 0.0001$, $P = 0.0015$). *$P < 0.05$, **$P < 0.01$, ***$P < 0.001$, ****$P < 0.0001$. **b**, The residual-P releasing ability of the soil microbial community in surface soil under Al+ and Al + RP. $n = 100$ individual cells. The two-sided unpaired *t*-test method was used for statistical significance testing ($P < 0.0001$). ****$P < 0.0001$. **c**, Rhizosphere in situ phosphatase activity. Scale bar, 2 cm. **d**, Top 15 *phoD*-harbouring bacterial genera in the surface rhizosphere soil at the elongation stage. The underline indicates the genus to which SynCom belongs. The red arrow represents the abundance of the genus *Pseudomonas*, which increased in Al + RP compared with Al+. $n = 3$ biological replicates. **e**, Transmission electron microscopy images of *R. erythropolis* and Raman spectra of the polyP band of *R. erythropolis* observed at 1,170 cm^{-1} under 0 mM, 0.1 mM and 1.0 mM Al^{3+} conditions for 24 h at 30 °C. $n = 30$ individual cells. The red arrow represents the oligobody composed of polyP. The two-sided unpaired *t*-test method was used for statistical significance testing ($P = 0.0003$, $P = 0.0046$). **$P < 0.01$, ***$P < 0.001$. In **b** and **e**, the horizontal bars in box plots represent medians. The tops and bottoms of the boxes show the 75th and 25th percentiles, respectively. The whiskers extend to minimum and maximum value.

Taken together, rice plants growing in association with SynCom formed longer, thinner and shallower roots in acidic soil relative to those growing in isolation or with traditional lime application. We inferred that this may be related to the changes in Al content and nutrients in the soil profile because the variation in root architecture, especially the shallow root type, is generally considered the response of plants to stress alleviation and a strategy for P acquisition[25].

SynCom-mediated reduction in Al toxicity

Given the reduced Al toxicity inferred from root elongation, we analysed the changes in pH and Al^{3+} content along the soil profile. With SynCom inoculation, the surface soil pH increased significantly from 5.15 to 5.79, accompanied by a decrease in the Al^{3+} content from 0.53 to 0.19 mg l^{-1} (0–4 cm) (Fig. 3a). Meanwhile, the SynCom members were enriched in the surface soil, as detected by qPCR (Fig. 3b).

To verify whether SynCom establishes crosstalk with plants and the impact on the microbial community that is directly associated with plants, we used DNA stable-isotope probing (DNA-SIP) to distinguish the rhizosphere bacterial groups that metabolized ^{13}C-labelled root exudates (Fig. 3c). Unconstrained principal coordinate analysis revealed that the bacterial community taking up root-derived carbon was significantly changed by SynCom inoculation. At the genus level, *Pseudomonas* was highly enriched with ^{13}C, implying that these bacteria utilized plant photosynthesis and exuded ^{13}C in the rhizosphere (Fig. 3d). *Rhodococcus* was also ^{13}C labelled but much less enriched (Fig. 3e). qPCR showed that the relative abundances of ^{13}C-labelled *R. erythropolis* and *P. aeruginosa* in Al + RP increased by 11.4% and 35.7%, respectively, compared with those in Al+ (Supplementary Fig. 16). Network analysis showed that the relationship among *Rhodococcus*, *Pseudomonas* and other taxa became simpler with SynCom inoculation in both the ^{12}C and ^{13}C groups (Supplementary Fig. 17). *Rhodococcus* was positively linked to *Phormidium IAM M-71*, while *Pseudomonas* consistently had negative links with *Conexibacter*, *Acidothermus* and *JG30a-KF-32 I*. SynCom inoculation also shifted the microbial community composition, with increased abundances of rhizosphere P-solubilizing bacteria *Bacillus*, *Clostridium*, *Chryseobacterium* and *Flavobacterium* in the ^{13}C-labelled communities (Al + RP versus Al+) (Supplementary Fig. 18). Among them, *Flavobacterium* has recently been reported to possess a phosphate-insensitive phosphatase, PafA, for rapid organic P remineralization[26].

To identify the possible mechanism by which SynCom inoculation elevated soil pH, we investigated the extracellular protonation process of *P. aeruginosa*, one of the SynCom members that mainly utilizes rhizodeposited carbon. The results of Fourier transform infra-red spectroscopy and zeta potential analysis showed that the protonation of bacterial organic anions is responsible for inhibiting acidification in soil (Fig. 3f and Supplementary Fig. 19). The abundant organic anionic functional groups (-COO^- or -O^-) on the surface of *Pseudomonas* interact with protons (H^+) to form neutral molecules[27]. The reactions of these functional groups can be reflected in shifted bands on the absorbance spectrum of the *P. aeruginosa* suspension (Fig. 3f and Supplementary Text 2.4). SynCom increased the Al resistance capacity of soil active bacteria by 47.7% and 105.6% under 0.3 mM and 0.5 mM Al^{3+} (pH 4.0), respectively, indicating a revival of microbial community activities (Supplementary Fig. 20). With increasing pH in surface soil, Al^{3+} was chelated and immobilized, thus reducing the toxicity to both plant and rhizosphere microorganisms. Although Al^{3+} increased with SynCom in the subsoil (9–10 cm) possibly due to the decomposition of Al-P compounds by more phosphatase and a small amount of Al leaching, the deeper rice roots were less susceptible to Al with SynCom inoculation (Supplementary Fig. 21).

SynCom promotes surface soil P mobilization

To determine whether the transition to shallow roots after SynCom inoculation was related to P availability, we performed sequential extraction to determine the P forms and fractions along the soil depth profile (Fig. 4a). Inoculation with SynCom decreased the contents of organic P and residual P by 61.1% and 9.51%, respectively, in the topsoil (0–4 cm), while there was no difference in the amount of available P at this depth. Through the diffusive gradients in the thin film method, we confirmed that the available P in situ was scarcely different (Supplementary Fig. 22). This suggested that organic P and residual P in topsoil were decomposed or solubilized and utilized. Additionally, we found that after mixing the acidic soil uniformly with exogenous P, the root length, diameter and tips no longer changed with SynCom (Supplementary Text 2.3 and Supplementary Fig. 23).

SynCom improved the residual P solubilization activity of topsoil bacterial communities by 37.2%, as quantified by the C–D ratio from Raman-D_2O spectroscopy (Fig. 4b). Acid phosphatases (ACPs) and alkaline phosphatases (ALPs), produced mainly by plants and microorganisms, respectively, contribute to the mineralization of organic P (ref. 28). We measured both ACPs and ALPs in the soil profiles by in situ soil zymography (Fig. 4c). SynCom significantly stimulated ALP activity, especially in the surface soil layer at 2–4 cm, and restored the activity of root-derived ACPs to some extent. This indicated that the microbial communities and microbial-derived ALP activities were crucial in the mineralization of organic P in topsoil. The *phoD* gene is considered the key ALP-encoding gene in soil and is widely used as a biomarker of ALP-encoding microbial communities[29]. We then analysed the composition of *phoD*-harbouring bacteria and found that *Pseudomonas*, as the most abundant *phoD*-harbouring taxon, obviously increased after SynCom inoculation (Fig. 4d). The relative abundance of *Pseudomonas* increased from 0.0087% to 9.17%. In addition, the relative abundance of *Rhodococcus* carrying the *phoD* gene increased from 0.0015% to 0.016%.

Interestingly, we found a potential unique function of *R. erythropolis* (a member of the SynCom) in mediating soil P availability under Al stress. Transmission electron microscopy analysis showed that *R. erythropolis* formed an oligobody composed of polyphosphate (polyP) (Fig. 4e). The polyP accumulation capacity of *R. erythropolis* increased by 46.6–55.2% under Al stress (pH 4), as indicated by the significantly elevated peak at 1,170 cm^{-1} (ref. 30). This intracellular structure is involved in the storage of P, pH homeostasis, osmoregulation and stress response under oligotrophic conditions[31]. In addition, at the transcriptome level, we found that Al stress increased the expression of genes encoding polyP synthesis, accumulation and depolymerization in *R. erythropolis* (Supplementary Fig. 24a). The genes involved in this pathway include *PPK1* and *PPK2*, encoding polyphosphate kinases; *PPX*, encoding an exopolyphosphatase; and *PPGK*, encoding the polyphosphate glucokinase that phosphorylates glucose using polyP to further release phosphate[32]. Meanwhile, Al-resistant *P. aeruginosa* highly expressed organic P mineralization-related genes (Supplementary Fig. 24b), which possibly established an association by providing more phosphate for *R. erythropolis* to restore and release.

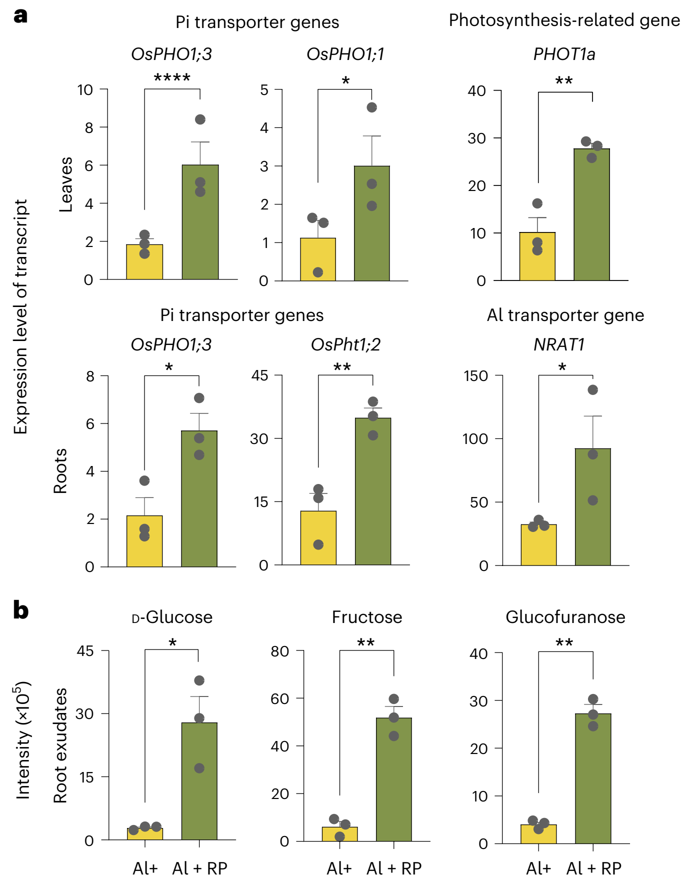

Fig. 5 | Enhanced Al-resistant response in rice provides more carbon for the root microbiota. a, SynCom promotes the expression of genes related to phosphorous starvation, photosynthesis and Al transporters in rice leaves and roots. **b**, The secretion of root exudates in the soil system. Data are presented as mean ± s.e.m. of three biological replicates. The two-sided unpaired *t*-test method was used for statistical significance testing (D-glucose, $P = 0.0143$; fructose, $P = 0.0008$; glucofuranose, $P = 0.0002$). *$P < 0.05$, ***$P < 0.001$. In **a**, the resulting *P* values were adjusted using Benjamini and Hochberg's approach for controlling the false discovery rate. Leaves: *OsPHO1;3*, $P_{adj} = 0.0001$; *OsPHO1;1*, $P_{adj} = 0.0287$; *PHOT1a*, $P_{adj} = 0.0054$. Roots: *OsPHO1;3*, $P_{adj} = 0.0126$; *OsPHO1;2*, $P_{adj} = 0.0213$; *NRAT1*, $P_{adj} = 0.0483$). *$P_{adj} < 0.05$, **$P_{adj} < 0.01$, ****$P_{adj} < 0.0001$.

'C–P' exchange between the root microbiota and rice

Predictably, the more abundant P in topsoil coupled with a shallow root type promoted phosphate transport in rice plants. For example,

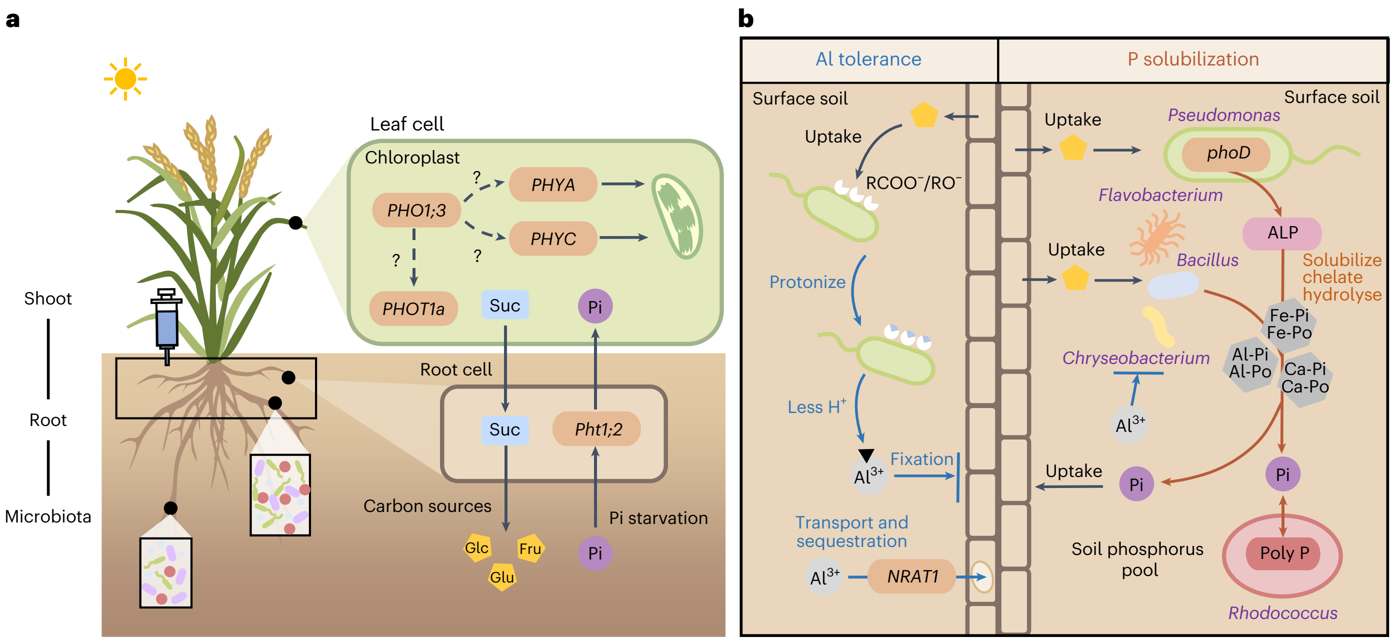

Fig. 6 | A schematic model summarizing the hypothesized mechanisms of how SynCom confers rice Al resistance and plant growth in acidic soil. a, Rice under Al-toxic acidic stress with SynCom. SynCom promotes photosynthesis and stimulates the transfer of sucrose (Sucs) from shoots to roots, thus promoting root exudate secretion. The monosaccharides in root exudates, including glucose (Glu), fructose (Fru) and glucofuranose (Glc), provide carbon sources and energy for rhizosphere microbial communities. The root architecture is modified to increase P uptake and transport from roots to shoots. Pi transporter genes, *OsPHO1;3* (*PHO1;3*) and *OsPht1;2* (*Pht1;2*); phototropin gene, *PHOT1a*; phytochrome genes, *PHYA* and *PHYC*. **b**, Al-tolerance and P-solubilization process in surface soil. The protonation of bacterial organic anions on adhered bacteria, such as *Pseudomonas*, inhibits the production of soil soluble Al and exchangeable Al, resists the decline in pH and Al toxicity, and retards soil acidification. P-solubilizing microorganisms, such as *Pseudomonas*, can mobilize insoluble Pi and Po compounds to soluble Pi by ALP for plant and microorganism uptake. P-accumulating microorganisms, such as *Rhodococcus*, can store Pi in the form of polyP and release Pi for plant uptake. SynCom recruits Al-sensitive P-solubilizing rhizosphere microbiota, which can cooperate to enrich the source of available P. ALP gene, *phoD*; Al transporter gene, *NRAT1*.

the expression of *OsPHO1;3* and *OsPHO1;1* increased significantly in leaves, and that of *OsPHO1;3* and *OsPht1;2* increased in roots (Fig. 5a). The *OsPht1;2* gene is reported to be essential for the long-distance transport of phosphate from roots to shoots[33]. We found that SynCom significantly reduced the root:shoot ratio of the P content by 50.2% (Supplementary Fig. 25a). In addition, the increased expression of *NRAT1* contributed to rice Al resistance (Fig. 5a). *NRAT1* is a plasma membrane-localized transporter for Al^{3+}, which is required for a prior step of final Al detoxification through sequestration into vacuoles[34]. Concomitantly, the expression of the phototropin gene *PHOT1a*, the phytochrome genes *PHYA* and *PHYC*, and sucrose transporter gene *OsSUT4* significantly increased (Supplementary Fig. 25b). Our results showed that SynCom enhanced photosynthesis and long-distance transport of sucrose for robust root growth. All these results suggested that the functional coordination between SynCom and root microbiota benefited rice growth in acidic soil. In return, the root secretes more monosaccharides as exudates, including glucose, fructose and glucofuranose, for rhizosphere microbes as carbon source (Fig. 5b and Supplementary Table 3). Thus, positive feedback between the root microbiota and plants was established through 'C–P' exchange.

Discussion

Soil–plant–microbe interactions are crucial for plant health[10,11]. Here we revealed how root microbiome could influence plant health in acidic soil with Al toxicity (Fig. 6a). First, we found that SynCom, consisting of highly Al-resistant bacterial isolates, decreased the Al^{3+} content by retarding acidification of the surface soil through protonation. This process reduced the risk of plant root tissue and microbe exposure to Al toxicity. Then, SynCom synergized with the native microbiota, in the release of phosphate from residual P and organic P in the topsoil (Fig. 6b). Plants optimized root architecture into shallow, P capture-favouring types[25], enhancing phosphate absorption and transport, photosynthesis and sucrose transport from shoots to roots (Fig. 6a). Proportionally more carbon may be allocated to roots to maintain robust root growth and exudation. Root exudates provide various carbon and energy sources for maintaining beneficial microbes[35], including inoculated SynCom members.

Raman-D_2O spectroscopy is an appealing culture-independent approach for elucidating metabolic activity at the single-cell level[36]. This method provides promising ways to improve the design of Al-resistant SynCom based on our current work. A higher-throughput protocol for screening Al-resistant strains from native soil may enlarge the candidate pool and optimize the SynCom design. As fungi and other eukaryotes are functionally important microbes in promoting soil and plant health[37], their interkingdom interactions with bacteria, and roles in conferring plant Al resistance need to be further evaluated. Further work is required to evaluate stress-resistant microbiota, including diverse members from bacteria, fungi and other taxa, in complex agricultural systems and to assess the long-term influence of SynCom inoculation on soil structure and functions[38,39].

Expanding the application of microbial products (single-strain or reduced-complexity consortia) from laboratory to field trials to promote plant health and stress tolerance remains challenging[40]. One major barrier is the quick out-competition of microbial inoculants by the resident community[39]. In this study, SynCom members were isolated from the rice rhizosphere and were shown to be recruited by rice roots and capable of occupying a stable niche after inoculation, especially *P. aeruginosa*. This may be due to their ability to strengthen soil functions by establishing crosstalk between the root microbiota and plants by trading P for plant photosynthetic carbon. These observations suggested that re-introducing native species rather than adding exotic species may promote the establishment success and survival of inoculants in plant–soil systems[38,39]. Therefore, screening resident microorganisms for targeted functions as microbial inoculants may be a viable measure to design microbial products that improve agroecosystem functioning and combat other abiotic stresses[41]. However, the plant molecular bases for recruiting SynComs, such as whether there is one or more quantitative trait loci in rice to enrich the specific SynCom, require further study.

Soil acidification and Al toxicity are among the biggest obstacles to crop production worldwide[1]. Agricultural liming has been a common practice for centuries to prevent soil acidification and the release of Al and potentially toxic metals into soil waters and plants[24]. However, such large-scale agricultural practices are restricted due to economic considerations and soil compaction caused by liming[42]. Our study demonstrated that rice exhibited better growth in the presence of native SynCom inoculation under Al stress than with traditional lime application. This could be because the application of limestone lowers the soil aggregate stability[43], accelerates the loss of mineral nutrients[44], and thus exacerbates the nutrient deficiency in acidic soils in the long term. Furthermore, liming leads to dramatic disturbance of the composition of native microbial communities[45], whereas inoculating with indigenous species has a milder impact[13]. This microbial strategy can be exploited as a safe, sustainable approach with a less adverse impact on the environment. More data are required to evaluate the long-term effects of SynCom inoculation on soil structure and functions in agricultural systems[39,46].

Phosphorus security is emerging as one of the twenty-first century's greatest global sustainability challenges, and its inefficient use across the whole food system is threatening the growing food demand[47]. Low phosphorus availability affects over 60% of the land currently used for agriculture, especially in acidic soils in tropical and subtropical regions of the world. Phosphorus use efficiency in crop production needs to be improved in P-fixing soil[48]. SynCom-induced 'C–P' exchange between plants and the microbiota contributes to the mineralization of organic P and solubilization of residual P. The functional coordination between plants and microbes offers a promising way to increase the usage of legacy P in soil, thereby reducing the need for P fertilizer input in agricultural stress-prone areas.

Collectively, our work indicated that applying an Al-resistant SynCom considerably improved rice Al resistance and alleviated P deficiency. The inoculated SynCom taxa that persisted in high abundance in the rhizosphere increased pH and decreased Al^{3+} via protonation, promoted ALP, and reduced the root growth angle for P acquisition in the topsoil. The interdependence of rice plant performance, root microbiome composition and edaphic conditions highlights the need to consider the internal integrity in plant–soil–microbiota in agroecosystems. Taking advantage of microbial strategies such as customized SynComs for sustainable agriculture is a promising method to improve plant growth, yield and resistance.

Methods

Cultivation of rice root microbiota

Rhizosphere soil samples were collected from the Yingtan Agro-ecosystem Field Experiment Station of the Chinese Academy of Sciences (28° 15′ 20″ N, 116° 55′ 30″ E). The rhizosphere soil pH was approximately 4.86 with an Al^{3+} content of 0.62 mg l^{-1}. Three healthy rice plants at the tillering stage, including roots, were excavated from each plot in the field, sealed in a polyethylene wrapper and brought back to the laboratory on ice. Microbial strains isolated from rhizosphere soil samples were obtained by the standard serial dilution culture method (Supplementary Methods). A total of 421 isolates were isolated, and 248 unique strains were purified several times using lysogeny broth (LB) medium before an individual colony was obtained (Supplementary Table 1). Microbial isolates were then identified by blasting against the National Center for Biotechnology Information database with the full-length 16S rRNA gene obtained from Sanger sequencing (Supplementary Methods). A maximum likelihood tree was constructed using MEGA 11 and R 4.2.1. The relative abundance of each species was obtained from 16S rRNA correlation analysis. Representative amplicon sequence variants (ASVs) were identified from the microbiome sequencing data of the field soil from which they were isolated. The matching ASVs displaying >97% sequence identity with the sequence of the full length of the 16S rRNA gene of each strain were kept as matched ASVs.

Growth media with $AlCl_3{\cdot}6H_2O$ supplementation

The availability of free Al^{3+} and how it reacts with other available ligands in soil solution or nutrient growth media is highly dependent on pH (ref. 49). To avoid Al precipitation, the pH for growth media used in this study was pre-adjusted to 7.8 with KOH before adding $AlCl_3{\cdot}6H_2O$, and the final pH was adjusted to 4.0 with HCl[50]. Three replicates were used for each Al^{3+} added concentration. For undefined LB medium, we determined the Al^{3+}, available P and other elements to consider the potential chelation and complexation between metal ions and other ligands using inductively coupled plasma–optical emission spectrometry (PerkinElmer Avio 200) analysis (Supplementary Table 4a and Supplementary Methods). For both LB and other defined media, calculation of theoretical ligand interactions and actual free Al^{3+} in LB medium were estimated by Geochem-EZ provided by Dr Jon E. Shaff and Dr Eric J. Craft[51] (Supplementary Table 4b). These data proved that our experiments were set up with Al stress under the correct acidic pH.

Identification of Al-resistant strains by Raman–D_2O

The representative strains were selected from the main branches in the phylogenetic tree, and their relative abundance ranked in the top 3 in the corresponding branches. Twelve representative bacteria stored at −80 °C were cultivated overnight in LB media. To quantify D substitution in C − H bonds, the intensities of the C–D peak (2,040–2,300 cm^{-1}) and the C–H peak (2,800–3,100 cm^{-1}) were used to calculate the C–D ratio of CD/(CD + CH). Five microlitres of bacterial suspension was incubated in 5% D_2O LB medium amended with 0 mM or 5 mM $AlCl_3{\cdot}6H_2O$ for 18 h in 96-well microtitre plates before Raman spectroscopy (Supplementary Methods).

Evaluation of Al-resistant ability

Single colonies of D95 and D65 were streaked onto LB agar plates and cultivated for 24–48 h at 30 °C. Pure cultures of the strains were cultured overnight in 5 ml LB medium. Twenty-five microlitres of each bacterial suspension was inoculated into 175 µl LB medium with different Al^{3+} added conditions (0, 0.1, 0.3, 0.5, 1.0 mM, final pH 4.0) in 96-well plates. Six replicates were used for each treatment. OD_{600} was measured every hour for 48 h at 30 °C (Bioscreen C Automated Growth Curve Analysis System, Oy Growth Curves Ab Ltd). The microbial growth curve model (logistic growth model) was constructed by Origin 2021.

Preparation of SynCom

A SynCom was derived from two efficient Al-resistant strains: *R. erythropolis* (Rh) and *P. aeruginosa* (Ps). The *P. aeruginosa* used in this study was preliminarily identified as a nonhuman opportunistic pathogen (Supplementary Methods). Two hundred microlitres of each bacterial suspension from *R. erythropolis* and *P. aeruginosa* stored at −80 °C was cultured in 50 ml of LB liquid medium and incubated at 30 °C and 180 rpm in a rotary incubator. When the OD_{600} of bacterial suspensions reached 0.6–0.8 during the exponential growth phase, the streak plate technique was used for isolation into a pure culture. SynCom was obtained by inoculating the two prepared bacterial suspensions in equal volumes (Supplementary Methods). In the field and pot experiments, 3 days after transplantation, 25 ml of the SynCom suspension was inoculated into the root zone of each rice seedling with a sterile syringe.

Rice germination and plant traits

Rice seeds from Nanjing 46 (*japonica*), Shanhanzinuo (*indica*), Jinguoyin (*indica*) and Nipponbare (*japonica*) were surface sterilized in 75% ethanol for 30 s and 2.5% sodium hypochlorite three times for 15 min and germinated on Murashige and Skoog (MS) agar media for 15 days (25 °C). Seedlings from each rice variety grown on MS agar media were selected and transplanted to plots in the field or pots in the greenhouse. Photographs of rice plants were taken by a digital camera (Ricoh GRIII, R02010), and plant height and chlorophyll content (SPAD-502 Plus, Konica) were periodically measured. Root and shoot fresh weights were measured after sampling. Root and shoot dry weights were measured after being dried to a constant weight in an oven at 65 °C. Single panicle weight was determined after harvest.

Field experiment

Rice seedlings from Nanjing 46 were selected and transplanted to the experimental field at the Yingtan Agroecosystem Field Experiment Station of the Chinese Academy of Sciences. The measurements of physicochemical properties are described in Supplementary Methods. (Supplementary Table 5). A total of 24 rice seedlings were transplanted into one plot (1.5 m × 3 m) at equal intervals. Plants on the borders of the plots were designated for protection and were not harvested. Each plot was randomly arranged, and each treatment had four biological replicates. The field experiment was managed following local conventional tillage.

Preliminary experiment of plant growth promotion

Rice seedlings from Nanjing 46 were selected and transplanted to pots (4 cm in length × 4 cm in width × 10 cm in depth) filled with 145 g collected field soil. Each pot contained one rice seedling. Plants were grown in a greenhouse under natural light conditions and kept flooded. The pot experiment was set up with or without microbial inoculations under Al stress conditions (control check, monocultures of *R. erythropolis* and *P. aeruginosa*, and SynCom named as RP). Plant samples were collected at the elongation stage.

Pot experiment conducted over the complete growth period

Seedlings of *japonica* Nanjing46 and Nipponbare and *indica* Shanhanzinuo and Jinguoyin were selected and transplanted to pots. The pot experiment was set up with or without SynCom under Al stress conditions (Al+, Al + RP) and limed soil conditions (LS, LS + RP). The limed soil condition was set up with 0.156 g $CaCO_3$ per 100 g acidic soil. The peroxidase activity in rice root tissue was measured using an assay kit (Suzhou Comin Biotechnology Co., Ltd.) according to the manufacturer's instructions. Fluorescence was detected by a spectrofluorometer (WFZ UV-2000).

Pot experiment with P supplementation

Rice seedlings from Nanjing 46 grown on MS agar media were transplanted to pots filled with a total of 145 g soil amended with 0.052 g calcium superphosphate per 100 g limed soil. Plant and root samples were photographed and collected at the elongation stage. Root morphology analysis was carried out at the mature grain stage.

Plant growth promotion assay in a clay-based system

Surface-sterilized and germinated seedlings of *japonica* Nanjing46 were transplanted into tissue culture bottles containing 200 g of calcined clay and 250 ml of modified Magnavaca's nutrient solution (1.0 mM KCl, 1.5 mM NH_4NO_3, 1.0 mM $CaCl_2$, 200 µM $MgSO_4$, 500 µM Mg $(NO_3)_2$, 155 µM $MgCl_2$, 11.8 µM $MnCl_2{\cdot}4H_2O$, 33 µM H_3BO_3, 3.06 µM $ZnSO_4{\cdot}7H_2O$, 0.8 µM $CuSO_4{\cdot}5H_2O$, 1.07 µM $Na_2MoO_4{\cdot}H_2O$ and 77 µM Fe-HEDTA). The calcined clay was washed with water, sterilized three times by autoclaving and heat-incubated until completely dehydrated. Four experimental factors were included: with or without SynCom inoculation, pH (4.0 and 6.0), Al^{3+} concentration (0.0, 0.1 and 0.5 mM), and available P (0.5, 2.5, and 6 mg l^{-1}). Different P conditions were provided by KH_2PO_4. Solution ion activities were estimated to consider the potential chelation and complexation using Geochem-EZ (Supplementary Table 4c)[51]. At pH 4.0, free Al^{3+} existed at 0.1 mM and 0.5 mM under different P concentrations. At pH 6.0, Al precipitated, and free Al^{3+} did not exist[49].

The plant growth promotion assay was carried out as a completely random experimental design, including a total of 36 treatments with 3 parallel biological plants in every tissue culture bottle and 4 replicates for each treatment. The OD_{600} of SynComs was adjusted to 0.5, and 2 ml SynCom was added to the clay-based system per plant (~10^6 cells per gram of calcined clay). Plants were grown at 30 °C under 12 h of light. After 2 weeks, plant height was measured to evaluate plant growth promotion.

Distribution of Al in root tissue

The root samples (Al+ and Al + RP) of Nanjing 46 rice in the pot experiment were collected at the elongation stage. The Al in roots was confirmed by energy-dispersive X-ray spectroscopy. The distribution of Al in the roots was determined by transmission electron microscopy (Supplementary Methods).

Soil zymography, soil pH and P stratified measurement

Soil zymography in situ was used to quantify the ACP and ALP enzyme activities in paddy soil (Supplementary Methods). After 40 min of dark culture, the membranes used for visualizing the activities of ACP and ALP were separated, dried for 10 min, and photographed. The enzyme concentration value was calculated on the basis of the greyscale intensity of the scanned images. Then, stratified soil samples were taken (1 cm per soil layer, ten layers per pot). After air-drying, the soil pH was determined. Stratified soil P measurements were performed by sequential extraction to quantify the amount of available P, primary P, secondary P organic P and residual P (ref. 52).

Measurement of Al^{3+} and available P using DGT in situ

The levels of Al^{3+} and available P in the rhizosphere soil of Nanjing 46 rice in the pot experiment (Al+, Al + RP, $n = 3$) at the elongation stage were estimated using the in situ diffusive gradients in thin films technique (DGT) (Supplementary Methods). The DGT probes used in this study were manually inserted into the rice root zone of soils with the least possible disturbance to the root zone. The probes were retrieved after 24 h and transferred to the laboratory for analyses.

2D visualization of root morphology

Collected plants, including rice roots at the mature grain stage, were shaken to remove the loosely adhering soil, and then washed with de-ionized water to remove soil attached to the surface; the roots were placed in a Petri dish filled with water and spread out with tweezers. Root morphology was scanned using Expression 11000XL (EPSON). Then, the root length, root diameter, root surface area, root volume, root crossing, root folks and root tip number of each rice variety were obtained using the WinRHIZO PRO LA2400 scanner system and software (Regent Instruments, Inc.). Dried shoot and root samples, grain weight per panicle and root:shoot ratios were measured.

3D visualization of root architecture in situ

3D X-ray computed tomography (CT) was used to visualize the root system architecture of Nanjing 46 rice at the elongation stage beneath the soil at Al+, Al + RP, LS, and LS + RP. Rice roots were scanned using the X-ray CT system (Phoenix Nanotom S) (Supplementary Methods).

Rhizobox experiment and root drawing in situ

Rice seedlings from Nanjing 46 were transferred and grown in the rhizobox system in a greenhouse with 520 g limed soil (15 × 1.5 × 18 cm) and maintained under flooding conditions. Each rhizobox contained one plant and was kept inclined at an angle of 45° to ensure that the roots could grow along the lower side covered with a blackout fabric. The roots on the image were marked using Photoshop, and then the root angle was calculated.

Alleviating effect of *P. aeruginosa* on soil acidification

Potential of *P. aeruginosa* in elevating soil pH and alleviating Al toxicity was assessed by zeta potential measurement and Fourier transform infra-red spectroscopy (Supplementary Methods). Each treatment had three biological replicates.

SIP incubations

^{13}C labelling was started when Nanjing 46 rice was in an active vegetative growth stage in Al+ and Al + RP ($n = 3$), and labelling was conducted over 21 days (Supplementary Methods). $^{13}CO_2$ was produced by the reaction between ^{13}C-Na_2CO_3 (99.99 atom% ^{13}C, 1 M) and HCl (1 M). A constant CO_2 concentration (450 µl CO_2 l^{-1}) inside the chamber was achieved via further automatic reactions. The plants were kept flooded, and rhizosphere soil samples were collected at the end.

Bacterial 16S rRNA processing

DNA was extracted from 0.5 g of each rhizosphere soil sample and purified on the basis of different buoyant densities and was subjected to 16S rRNA gene amplicon sequencing for each treatment. Briefly, the V4–V5 primers 515 F-Y (5′-GTGYCAGCMGCCGCGGTAA) and 926R (5′-CCGYCAATTYMTTTRAGTTT) were used to design variable barcodes[53], and 16S rRNA gene fragments were amplified. The products were pooled and sequenced on the Illumina NovaSeq 6000 250 bp paired-end sequencing platform. Representative reads were picked using the DADA2 denoising algorithm ('q2-dada2' plugin) to generate an ASV table. Taxonomy was assigned to each ASV by comparing the representative sequences with the FunGene database[54]. Co-occurrence networks were constructed by calculating Spearman correlation coefficients using the R package 'igraph', and correlations with $r > 0.5$ and $P < 0.05$ were included in the network.

The *phoD* gene and the *phoD*-harbouring microbial community

Real-time qPCR of *phoD* gene abundance was performed on an ABI 7500 (Applied Biosystems) using rhizosphere soil collected at elongation stage of Nanjing 46 rice (Al+, Al + RP, $n = 3$) growing in the pots. An Omega Soil DNA Kit (CAT: M5635-02) was used to extract DNA from the soil samples. The primers ALPS-F730 (5′-CAGTGGGACGACCACGAGGT-3′) and ALPS-R1101 (5′-GAGGCCGATCGG-CATGTCG-3′) were used to amplify bacterial *phoD* genes[55]. The PCRs were prepared as described previously[56]. The communities of *phoD*-harbouring bacteria were assessed using the Illumina NovaSeq 6000 250 bp paired-end sequencing platform. The sequencing procedure was the same as described above.

Determination of the P-releasing ability of soil bacteria

Rhizosphere soil samples from Nanjing 46 at the elongation stage in the pot experiment (Al+, Al + RP, $n = 3$) were collected to determine the P-releasing ability of the soil bacteria. A modified Nycodenz density-gradient separation protocol from previous reports was used to extract bacteria from soil[57,58]. The as-prepared bacteria were inoculated in 50 ml of 50% (v/v) D_2O MM-Ca_3P medium (10 g l^{-1} glucose, 0.5 g l^{-1} $(NH_4)_2SO_4$, 0.3 g l^{-1} KCl, 0.3 g l^{-1} NaCl, 0.03 g l^{-1} $MnSO_4{\cdot}H_2O$, 0.03 g l^{-1} $FeSO_4{\cdot}7H_2O$, 0.03 g l^{-1} $MgSO_4{\cdot}{}_7H_2O$ and 2.5 g l^{-1} $Ca_3(PO_4)_2$, final pH 4.0) for 24 h at 28 °C (ref. 58). All bacterial samples were washed with ultrapure water three times to remove residual media. The activity of soil bacteria was determined by Raman–D_2O.

Al resistance of the rhizosphere soil microbial community

Soil bacteria were extracted by the modified Nycodenz density-gradient separation protocol[57,58]. The extracted soil bacteria were transferred into 50% D_2O MM medium (10 g l^{-1} glucose, 0.5 g l^{-1} $(NH_4)_2SO_4$, 0.3 g l^{-1} KCl, 0.3 g l^{-1} NaCl, 0.03 g l^{-1} $MnSO_4{\cdot}H_2O$, 0.03 g l^{-1} $FeSO_4{\cdot}7H_2O$, 0.03 g l^{-1} $MgSO_4{\cdot}7H_2O$, 0.5 g l^{-1} KH_2PO_4 and 1.5 g l^{-1} Na_2HPO_4, final pH 4.0) amended with 0, 0.3 or 0.5 mM Al^{3+} and incubated at 30 °C for 24 h before Raman analysis. The actual free Al^{3+} was 0.07 and 0.13 mM under 0.3 and 0.5 mM, respectively, as estimated by Geochem-EZ (Supplementary Table 4d).

Leaf and root RNA-seq analysis

Rice leaves and root samples from Nanjing 46 at the elongation stage in the pot experiment (Al+, Al + RP, $n = 3$) were collected for RNA extraction and mRNA sequencing. Each sample was ground into a fine powder with liquid nitrogen. RNA-sequencing (RNA-seq) libraries were prepared and sequenced on the Nova seq 6000 platform. Normalized read counts were obtained using fragments per kilo base of transcript per million mapped fragments. Differentially expressed genes were obtained on the basis of DESeq (http://www.bioconductor.org/packages/release/bioc/html/DESeq.html). An absolute value of $|\log_2$fold change$| > 0$ and P value <0.05 were used as the thresholds to judge the significance of gene expression differences.

Non-targeted plant metabolite profiling

Root exudates from Nanjing 46 rice at the elongation stage in the pot experiment (Al+, Al + RP, $n = 3$) were analysed by non-targeted plant metabolite profiling with gas chromatography coupled with mass spectrometry (GC–MS). The dataset obtained with the GC–MS analyses was imported into SIMCA software (version 16.0.2) to perform multivariate statistical analyses (Supplementary Table 3 and Supplementary Methods).

qPCR of *P. aeruginosa* and *R. erythropolis*

The abundance of SynCom members in ^{13}C–CO_2 isotope labelling experiment for both ^{12}C- and ^{13}C-groups, and pot experiment at different growth stages (Al+, Al + RP, $n = 3$) was measured by qPCR. DNA was extracted and purified from 0.5 g of each rhizosphere soil sample. The specific primers PsA-16sF and PsA-16sR, and the primers Rh-16sF and Rh-16sR were used to amplify the target regions in *P. aeruginosa* and *R. erythropolis*, respectively (Supplementary Fig. 6 and Supplementary Methods).

Transcriptomics profiling of SynCom

Co-culture of *R. erythropolis* and *P. aeruginosa* was inoculated in KB medium amended with 0 mM or 0.1 mM Al^{3+} and grown in a rotary incubator (180 rpm) at 30 °C for 72 h to obtain enriched cultures. The total RNA of each sample was extracted using the RNeasy Plus Universal Mini Kit (Qiagen). RNA-seq libraries were sequenced on the Illumina NovaSeq 6000 platform, and 150 bp paired-end reads were generated. The raw data were processed with Trimmomatic (version 0.36) (ref. 59) and Bowtie2 (version 2.33) (ref. 60). Clean reads were mapped by HISAT2 onto the reference transcriptome. The transcriptomes were quantitatively analysed by RSEM software[61]. Differentially expressed genes were obtained based on 'edgeR' packages in R software.

Characterization of P accumulation in *R. erythropolis*

R. erythropolis was cultivated in liquid LB media (pH 4.0) for 5 days at 30 °C. A total of 3–4 mm *R. erythropolis* cells in a 1.5 ml eppendorf tube were collected by centrifuging 1 ml of bacterial solution for 5 min (4 °C, 10,000*g*) and repeated several times. Whole *R. erythropolis* cells were fixed in 1 ml 2.5% glutaraldehyde buffered at 4 °C for 2–4 h with three replicates. The sample processing procedure was the same as mentioned above before transmission electron microscope (JEM-1200EX) analysis at 120 kV.

The P accumulation ability of *R. erythropolis* was determined by Raman spectroscopy. *R. erythropolis* was cultivated in liquid LB media supplemented with 0 mM, 0.1 mM or 1.0 mM Al^{3+} for 24 h at 30 °C. All bacterial samples were washed with ultrapure water three times to remove residual media before single-cell Raman measurements following the procedure mentioned above. Peak intensity was quantified by calculating the peak area (polyP peak, 1,170 cm^{-1}). Data were calculated in R software.

Statistics and graphics

Data were statistically analysed and presented graphically using the R 4.2.1 statistical environment (https://cran.r-project.org/) or Prism 8.2.1 (GraphPad).

Reporting summary

Further information on research design is available in the Nature Portfolio Reporting Summary linked to this article.

Data availability

The raw sequence data reported in this paper have been deposited (PRJCA011216) in the Genome Sequence Archive in the BIG Data Center[62], Chinese Academy of Sciences under accession code CRA007891 for *Rhodococcus erythropolis* transcriptome sequencing, CRA007889 for *Pseudomonas aeruginosa* transcriptome sequencing, CRA008623 for bacterial 16S rRNA gene sequencing data in the ^{13}C isotope labelling experiment, CRA007869 for *phoD* gene sequencing, CAR007871 for rice leaf transcriptome sequencing, and CAR008056 for rice root transcriptome sequencing in the pot experiment and are publicly accessible at http://bigd.big.ac.cn/gsa. All pure strains were deposited in the CNGB Sequence Archive (CNSA)[63] of the China National GeneBank DataBase (CNGBdb)[64] at https://db.cngb.org/ with accession number CNP0003393. Source data are provided with this paper.

Code availability

The code used for this work is available from the corresponding author on request.

References

1. Kochian, L. V., Piñeros, M. A., Liu, J. & Magalhaes, J. V. Plant adaptation to acid soils: the molecular basis for crop aluminum resistance. *Annu. Rev. Plant Biol.* **66**, 571–598 (2015).
2. von Uexküll, H. R. & Mutert, E. Global extent, development and economic impact of acid soils. *Plant Soil* **171**, 1–15 (1995).
3. Yang, Z., Rao, I. M. & Horst, W. J. Interaction of aluminium and drought stress on root growth and crop yield on acid soils. *Plant Soil* **372**, 3–25 (2013).
4. Kochian, L. V., Hoekenga, O. A. & Piñeros, M. A. How do crop plants tolerate acid soils? Mechanisms of aluminum tolerance and phosphorous efficiency. *Annu. Rev. Plant Biol.* **55**, 459–493 (2004).
5. Siqueira, J. A., Silva, M. F., Wakin, T., Nunes-Nesi, A. & Araujo, W. L. Metabolic and DNA checkpoints for the enhancement of Al tolerance. *J. Hazard. Mater.* **430**, 128366 (2022).
6. Chandra, J. & Keshavkant, S. Mechanisms underlying the phytotoxicity and genotoxicity of aluminum and their alleviation strategies: a review. *Chemosphere* **278**, 130384 (2021).
7. Magalhaes, J. V., Piñeros, M. A., Maciel, L. S. & Kochian, L. V. Emerging pleiotropic mechanisms underlying aluminum resistance and phosphorus acquisition on acidic soils. *Front. Plant Sci.* **9**, 1420 (2018).
8. Kochian, L. V., Pineros, M. A. & Hoekenga, O. A. The physiology, genetics and molecular biology of plant aluminum resistance and toxicity. *Plant Soil* **274**, 175–195 (2005).
9. Delhaize, E., Ma, J. F. & Ryan, P. R. Transcriptional regulation of aluminium tolerance genes. *Trends Plant Sci.* **17**, 341–348 (2012).
10. Trivedi, P., Leach, J. E., Tringe, S. G., Sa, T. & Singh, B. K. Plant–microbiome interactions: from community assembly to plant health. *Nat. Rev. Microbiol.* **18**, 607–621 (2020).
11. Nerva, L. et al. Breeding toward improved ecological plant-microbiome interactions. *Trends Plant Sci.* **27**, 1134–1143 (2022).
12. Durán, P. et al. Microbial interkingdom interactions in roots promote *Arabidopsis* survival. *Cell* **175**, 973–983 (2018).
13. Narayanan, M. & Ma, Y. Metal tolerance mechanisms in plants and microbe-mediated bioremediation. *Environ. Res.* **222**, 115413 (2023).
14. Rajkumar, M., Sandhya, S., Prasad, M. N. & Freitas, H. Perspectives of plant-associated microbes in heavy metal phytoremediation. *Biotechnol. Adv.* **30**, 1562–1574 (2012).
15. Vorholt, J. A., Vogel, C., Carlström, C. I. & Müller, D. B. Establishing causality: opportunities of synthetic communities for plant microbiome research. *Cell Host Microbe* **22**, 142–155 (2017).
16. Zhang, J. et al. *NRT1.1B* is associated with root microbiota composition and nitrogen use in field-grown rice. *Nat. Biotechnol.* **37**, 676–684 (2019).
17. Carlström, C. I. et al. Synthetic microbiota reveal priority effects and keystone strains in the *Arabidopsis* phyllosphere. *Nat. Ecol. Evol.* **3**, 1445–1454 (2019).
18. Carrión, V. J. et al. Pathogen-induced activation of disease-suppressive functions in the endophytic root microbiome. *Science* **366**, 606–612 (2019).
19. Schmitz, L. et al. Synthetic bacterial community derived from a desert rhizosphere confers salt stress resilience to tomato in the presence of a soil microbiome. *ISME J.* **16**, 1907–1920 (2022).
20. Sukweenadhi, J. et al. *Paenibacillus yonginensis* DCY84^T induces changes in *Arabidopsis thaliana* gene expression against aluminum, drought, and salt stress. *Microbiol. Res.* **172**, 7–15 (2015).
21. Silambarasan, S., Logeswari, P., Cornejo, P., Abraham, J. & Valentine, A. Simultaneous mitigation of aluminum, salinity and drought stress in *Lactuca sativa* growth via formulated plant growth promoting *Rhodotorula mucilaginosa* CAM4. *Ecotox. Environ. Saf.* **180**, 63–72 (2019).
22. Gooderham, W. J. & Hancock, R. Regulation of virulence and antibiotic resistance by two-component regulatory systems in *Pseudomonas aeruginosa*. *FEMS Microbiol. Rev.* **33**, 279–294 (2009).
23. de Carvalho, C. C. C. R. & Da Fonseca, M. M. R. The remarkable *Rhodococcus erythropolis*. *Appl. Microbiol. Biot.* **67**, 715–726 (2005).
24. Goulding, K. W. T. & Blake, L. Land use, liming and the mobilization of potentially toxic metals. *Agr. Ecosyst. Environ.* **67**, 135–144 (1998).
25. Huang, G. et al. Rice actin binding protein RMD controls crown root angle in response to external phosphate. *Nat. Commun.* **9**, 2346 (2018).
26. Lidbury, I. D. E. A. et al. A widely distributed phosphate-insensitive phosphatase presents a route for rapid organophosphorus remineralization in the biosphere. *Proc. Natl Acad. Sci. USA* **119**, e2118122119 (2022).
27. Nkoh, J. N., Yan, J., Xu, R., Shi, R. & Hong, Z. The mechanism for inhibiting acidification of variable charge soils by adhered *Pseudomonas fluorescens*. *Environ. Pollut.* **260**, 114049 (2020).
28. Nannipieri, P., Giagnoni, L., Landi, L. & Renella, G. *Phosphorus in Action. Soil Biology* Vol. 26 (Springer, 2010).
29. Zimmerman, A. E., Martiny, A. C. & Allison, S. D. Microdiversity of extracellular enzyme genes among sequenced prokaryotic genomes. *ISME J.* **7**, 1187–1199 (2013).
30. Moudrikova, S. et al. Quantification of polyphosphate in microalgae by Raman microscopy and by a reference enzymatic assay. *Anal. Chem.* **89**, 12006–12013 (2017).

31. Yoshida, N. et al. A unique intracellular compartment formed during the oligotrophic growth of *Rhodococcus erythropolis* N9T-4. *Appl. Microbiol. Biot.* **101**, 331–340 (2017).
32. Zhong, C., Fu, J., Jiang, T., Zhang, C. & Cao, G. Polyphosphate metabolic gene expression analyses reveal mechanisms of phosphorus accumulation and release in *Microlunatus phosphovorus* strain JN459. *FEMS Microbiol. Lett.* **365**, fny034 (2018).
33. Paszkowski, U., Kroken, S., Roux, C. & Briggs, S. P. Rice phosphate transporters include an evolutionarily divergent gene specifically activated in arbuscular mycorrhizal symbiosis. *Proc. Natl Acad. Sci. USA* **99**, 13324–13329 (2002).
34. Li, J. et al. Natural variation underlies alterations in Nramp aluminum transporter (*NRAT1*) expression and function that play a key role in rice aluminum tolerance. *Proc. Natl Acad. Sci. USA* **111**, 6503–6508 (2014).
35. Vives-Peris, V., de Ollas, C., Gómez-Cadenas, A. & Pérez-Clemente, R. M. Root exudates: from plant to rhizosphere and beyond. *Plant Cell Rep.* **39**, 3–17 (2019).
36. Li, H. et al. Active antibiotic resistome in soils unraveled by single-cell isotope probing and targeted metagenomics. *Proc. Natl Acad. Sci. USA* **119**, e2093494177 (2022).
37. Frąc, M., Hannula, S. E., Bełka, M. & Jęyczka, M. Fungal biodiversity and their role in soil health. *Front. Microbiol.* **9**, 707 (2018).
38. Chen, Q. et al. Potential of indigenous crop microbiomes for sustainable agriculture. *Nat. Food* **2**, 233–240 (2021).
39. Hartmann, M. & Six, J. Soil structure and microbiome functions in agroecosystems. *Nat. Rev. Earth Env.* **4**, 4–18 (2023).
40. Saad, M. M., Eida, A. A., Hirt, H. & Doerner, P. Tailoring plant-associated microbial inoculants in agriculture: a roadmap for successful application. *J. Exp. Bot.* **71**, 3878–3901 (2020).
41. Singh, B. K., Trivedi, P., Egidi, E., Macdonald, C. A. & Delgado-Baquerizo, M. Crop microbiome and sustainable agriculture. *Nat. Rev. Microbiol.* **18**, 601–602 (2020).
42. Shaheen, S. M., Hooda, P. S. & Tsadilas, C. D. Opportunities and challenges in the use of coal fly ash for soil improvements—a review. *J. Environ. Manage.* **145**, 249–267 (2014).
43. Hammerschmitt, R. K. et al. Limestone and gypsum reapplication in an oxisol under no-tillage promotes low soybean and corn yield increase under tropical conditions. *Soil Till. Res.* **214**, 105165 (2021).
44. Gascho, G. J. & Parker, M. B. Long-term liming effects on coastal plain soils and crops. *Agron. J.* **93**, 1305–1315 (2001).
45. Sridhar, B. et al. Microbial community shifts correspond with suppression of decomposition 25 years after liming of acidic forest soils. *Global Change Biol.* **28**, 5399–5415 (2022).
46. Zhuang, X., Chen, J., Shim, H. & Bai, Z. New advances in plant growth-promoting rhizobacteria for bioremediation. *Environ. Int.* **33**, 406–413 (2007).
47. Cordell, D. & White, S. Life's bottleneck: sustaining the world's phosphorus for a food secure future. *Annu. Rev. Env. Resour.* **39**, 161–188 (2014).
48. Zou, T., Zhang, X. & Davidson, E. A. Global trends of cropland phosphorus use and sustainability challenges. *Nature* **611**, 81–87 (2022).
49. Kinraide, T. B. A. S. Identity of the rhizotoxic aluminium species. *Plant Soil* **134**, 167–178 (1991).
50. Famoso, A. N. et al. Development of a novel aluminum tolerance phenotyping platform used for comparisons of cereal aluminum tolerance and investigations into rice aluminum tolerance mechanisms. *Plant Physiol.* **153**, 1678–1691 (2010).
51. Shaff, J. E., Schultz, B. A., Craft, E. J., Clark, R. T. & Kochian, L. V. GEOCHEM-EZ: a chemical speciation program with greater power and flexibility. *Plant Soil* **330**, 207–214 (2010).
52. Tiessen, H. & Moir, J. O. *Soil Sampling and Methods of Analysis* Ch. 25 (Lewis Publishers, 1993).
53. Parada, A. E., Needham, D. M. & Fuhrman, J. A. Every base matters: assessing small subunit rRNA primers for marine microbiomes with mock communities, time series and global field samples. *Environ. Microbiol.* **18**, 1403–1414 (2016).
54. Fish, J. A. et al. FunGene: the functional gene pipeline and repository. *Front. Microbiol.* **4**, 291 (2013).
55. Sakurai, M., Wasaki, J., Tomizawa, Y., Shinano, T. & Osaki, M. Analysis of bacterial communities on alkaline phosphatase genes in soil supplied with organic matter. *Soil Sci. Plant Nutr.* **54**, 62–71 (2008).
56. Luo, G. et al. Understanding how long-term organic amendments increase soil phosphatase activities: Insight into *phoD*- and *phoC*-harboring functional microbial populations. *Soil Biol. Biochem.* **139**, 107632 (2019).
57. Eichorst, S. A. et al. Advancements in the application of NanoSIMS and Raman microspectroscopy to investigate the activity of microbial cells in soils. *FEMS Microbiol. Ecol.* **91**, fiv106 (2015).
58. Li, H. et al. D_2O-isotope-labeling approach to probing phosphate-solubilizing bacteria in complex soil communities by single-cell Raman spectroscopy. *Anal. Chem.* **91**, 2239–2246 (2019).
59. Bolger, A. M., Lohse, M. & Usadel, B. Trimmomatic: a flexible trimmer for Illumina sequence data. *Bioinformatics* **30**, 2114–2120 (2014).
60. Langmead, B. & Salzberg, S. L. Fast gapped-read alignment with Bowtie 2. *Nat. Methods* **9**, 357–359 (2012).
61. RSEM (RNA-seq by expectation-maximization). *GitHub* https://deweylab.github.io/RSEM (2018).
62. BIG, D. C. M. Database resources of the BIG Data Center in 2018. *Nucleic Acids Res.* **46**, D14–D20 (2018).
63. Guo, X. et al. CNSA: a data repository for archiving omics data. *Database* **2020**, baaa055 (2020).
64. Chen, F. et al. CNGBdb: China National GeneBank DataBase. *Hereditas* **42**, 799–809 (2020).

Acknowledgements

We thank J. E. Shaff and E. J. Craft (Robert W. Holley Center of Agriculture and health, USDA-ARS, Cornell University) for providing the helpful tool Geochem-EZ software. We thank C. Huang (Shanghai Center for Plant Stress Biology, Chinese Academy of Sciences) and G. Huang (School of Life Sciences and Biotechnology, Shanghai Jiao Tong University) for critical discussion and feedback on the paper. We thank J. Fan, M. Liu, X. Liu and L. Chen from the Yingtan Agroecosystem Field Experiment Station of the Chinese Academy of Sciences for field experiment management and sampling assistance. We received fundings from Strategic Priority Research Program of the Chinese Academy of Sciences (XDA24020104 to Y.L.), National Key R&D Program of China (2021YFD1900400 to Y.L.), National Natural Science Foundation of China (42377121 to Y.L.), Innovation Program of Institute of Soil Science (ISSASIP2201 to Y.L.) and Youth Innovation Promotion Association of Chinese Academy of Sciences (2016284 to Y.L.). The funders had roles in study design and data collection and analysis.

Author contributions

Conceptualization: Y.L., Y.B., T.W.C., R.S. and J. Zhang. Methodology: Y.L., C.L., M.J., M.M.Y., Z.M., Y.B., L.Z., Y.W., J.D., W.L. and J. Zhou. Investigation: Y.L., C.L., M.J. and M.M.Y. Data curation: C.L., M.J., M.M.Y., Z.M., L.Z. and J.D. Formal analysis: Y.L., C.L., M.J., M.M.Y., Z.M. and L.Z. Supervision: Y.L., E.W., R.S. and J. Zhang. Writing—original draft: Y.L., C.L., M.J. and M.M.Y. Writing—review and editing: C.L., M.J., M.M.Y., Y.L., E.W., Y.B., T.W.C., J. Zhou, Z.M., L.Z., Y.W., J.D., W.L., B.S., R.S. and J. Zhang.

Competing interests

The authors declare no competing interests.

Additional information

Supplementary information The online version contains supplementary material available at https://doi.org/10.1038/s43016-023-00848-0.

Correspondence and requests for materials should be addressed to Yuting Liang.

Peer review information *Nature Food* thanks Hongwei Liu, Miguel Pineros and Qing Yao for their contribution to the peer review of this work.

nature portfolio

Corresponding author(s): Yuting Liang

Last updated by author(s): Aug 30, 2023

Reporting Summary

Nature Portfolio wishes to improve the reproducibility of the work that we publish. This form provides structure for consistency and transparency in reporting. For further information on Nature Portfolio policies, see our Editorial Policies and the Editorial Policy Checklist.

Statistics

For all statistical analyses, confirm that the following items are present in the figure legend, table legend, main text, or Methods section.

n/a	Confirmed	
☐	☒	The exact sample size (n) for each experimental group/condition, given as a discrete number and unit of measurement
☐	☒	A statement on whether measurements were taken from distinct samples or whether the same sample was measured repeatedly
☐	☒	The statistical test(s) used AND whether they are one- or two-sided *Only common tests should be described solely by name; describe more complex techniques in the Methods section.*
☒	☐	A description of all covariates tested
☐	☒	A description of any assumptions or corrections, such as tests of normality and adjustment for multiple comparisons
☐	☒	A full description of the statistical parameters including central tendency (e.g. means) or other basic estimates (e.g. regression coefficient) AND variation (e.g. standard deviation) or associated estimates of uncertainty (e.g. confidence intervals)
☐	☒	For null hypothesis testing, the test statistic (e.g. F, t, r) with confidence intervals, effect sizes, degrees of freedom and P value noted *Give P values as exact values whenever suitable.*
☒	☐	For Bayesian analysis, information on the choice of priors and Markov chain Monte Carlo settings
☐	☒	For hierarchical and complex designs, identification of the appropriate level for tests and full reporting of outcomes
☐	☒	Estimates of effect sizes (e.g. Cohen's d, Pearson's r), indicating how they were calculated

Our web collection on statistics for biologists contains articles on many of the points above.

Software and code

Policy information about availability of computer code

Data collection	Root system architecture was segmented from the reconstructed images and visualized using Volume Graphics Studio (version 3.2). And the root length, diameter, and angle were measured by ImageJ 1.46 software (http://rsb.info.nih.gov/ij). In addition, all the Single-cell Raman spectra and attenuated total reflectance Fourier transform infrared (ATR-FTIR) spectrum were processed by LabSpec 5 and OMNIC 8.2 software to capture the corresponding band data, respectively.
Data analysis	R packages used: igraph and edgeR (version 4.2.1), Prism 8.2.1, Origin 2021, MEGA 11, Geochem-EZ (no version number), Excel and PowerPoint: Microsoft Office Home and Student 2019 were used for data analysis and visualization which were detailed in the manuscript.

For manuscripts utilizing custom algorithms or software that are central to the research but not yet described in published literature, software must be made available to editors and reviewers. We strongly encourage code deposition in a community repository (e.g. GitHub). See the Nature Portfolio guidelines for submitting code & software for further information.

Data

Policy information about availability of data

All manuscripts must include a data availability statement. This statement should provide the following information, where applicable:

- Accession codes, unique identifiers, or web links for publicly available datasets
- A description of any restrictions on data availability
- For clinical datasets or third party data, please ensure that the statement adheres to our policy

The raw sequence data reported in this paper have been deposited (PRJCA011216) in the Genome Sequence Archive in the BIG Data Center, Chinese Academy of Sciences under accession code CRA007891 for Rhodococcus erythropolis transcriptome sequencing, CRA007889 for Pseudomonas aeruginosa transcriptome sequencing, CRA008623 for bacterial 16S rRNA gene sequencing data in the 13C isotope labeling experiment, CRA007869 for phoD gene sequencing, CAR007871 for rice leaf transcriptome sequencing, and CAR008056 for rice root transcriptome sequencing in the pot experiment and are publicly accessible at http://bigd.big.ac.cn/gsa. All pure strains were deposited in the CNGB Sequence Archive (CNSA) of the China National GeneBank DataBase (CNGBdb) at https://db.cngb.org/ with accession number CNP0003393.

Human research participants

Policy information about studies involving human research participants and Sex and Gender in Research.

Reporting on sex and gender	N/A
Population characteristics	N/A
Recruitment	N/A
Ethics oversight	N/A

Note that full information on the approval of the study protocol must also be provided in the manuscript.

Field-specific reporting

Please select the one below that is the best fit for your research. If you are not sure, read the appropriate sections before making your selection.

☐ Life sciences ☐ Behavioural & social sciences ☒ Ecological, evolutionary & environmental sciences

For a reference copy of the document with all sections, see nature.com/documents/nr-reporting-summary-flat.pdf

Ecological, evolutionary & environmental sciences study design

All studies must disclose on these points even when the disclosure is negative.

Study description	Here, we isolated 248 bacterial strains from the rice rhizosphere in acidic red soils and developed an effective Al-resistant synthetic community (SynCom). The field and greenhouse experiments showed that SynCom increased rice performance in acidic soils. We aimed to develop an effective Al-resistant SynCom to promote plant growth under acidic Al toxicity condition and to explore the functional mechanism through plant-microbiome interactions. The key mechanism was that SynCom reduced Al toxicity in surface soil through bacterial extracellular protonation, synergized rhizosphere microbiota to expand the available P pool and induced shallow root development in rice for nutrient acquisition. In this study, for field experiment, we kept 4 biological replicate field plots. Three healthy rice plants at heading stage and mature grain stage were excavated from each plot in the field, that is, a total of 24 samples. In the pot experiment, n = 20 biological replicates of rice plants were evaluated for SPAD value, and n = 13 biological replicates of rice plants were measured for plant height. The biological replicates of other indicators were greater than 3.
Research sample	The soil samples were collected from the rhizosphere of japonica Nanjing 46 grown in an acidic field. In total, 248 unique microbial isolates were obtained using repeated plate streaking. We evaluated the Al-resistant activity of 12 representative strains. Rhodococcus erythropolis and Pseudomonas aeruginosa were the most resistant strains, which were combined as the SynCom for the subsequent microbial inoculation experiments. For pot experiment, the plant samples were taken from four rice varieties including japonica Nanjing46 and Nipponbare, indica Shanhanzinuo and Jinguoyin.
Sampling strategy	For soil samples: Rhizosphere soil samples were collected as follows: the loosely attached rhizosphere soil on the roots was removed with gentle shaking (shake-off method), and soil from within approximately 1-4 mm of the root was retained as rhizosphere soil and stored in the refrigerator at 4 °C. Rhizosphere soils for geochemical analyses were stored at 4 °C, and those for DNA extraction were stored at −80 °C. These soil samples were then used to investigate the diversity and composition of bacterial communities associated with the rice rhizosphere in acidic soils. For plant samples: Root and shoot fresh weights were measured after sampling. After analysis, dried shoot and root samples, grain weight per panicle, single panicle weight, and root:shoot ratios were then calculated.

Data collection	Soil pH was determined using a pH meter (Mettler Toledo, Switzerland) in a soil: water ratio of 1:2.5 (w/v). Soil organic carbon (SOC) was determined by potassium dichromate ($K_2Cr_2O_7$) oxidation with heating in an oil bath. The available nitrogen (N), P and potassium (K) in the soil were extracted by ammonium acetate. Soil micronutrient concentrations were measured using the diethylene-triaminepentaacetic acid (DTPA) extraction method. The soil mechanical composition was determined by the pipette method. Soil zymography was used to quantify the acid (ACP) and alkaline phosphatase (ALP) enzyme activities in paddy soil. Stratified soil phosphorus measurement was determined by sequential extraction. The content of Fe (II), Al (III), and available P in rhizosphere soil of Nanjing 46 rice in the pot experiment at the elongation stage were estimated using in-situ field application of the diffusive gradients in thin films (DGT) technique. Plant chlorophyll content was measured by chlorophyll meter (SPAD-502 Plus, Konica). Root morphology was scanned using Expression 11000XL (EPSON, Japan). Three-dimensional (3D) X-ray computed tomography (CT) was used to visualize root system architecture (RSA) of Nanjing 46 rice at the elongation stage. Distribution of Al in root tissue was analyzed with transmission electron microscopy (TEM). Root exudates from Nanjing 46 rice at the elongation stage in the pot experiment were analyzed by nontargeted plant metabolite profiling with gas chromatography coupled with mass spectrometry (GC–MS). DNA-SIP was used to identify the rhizosphere bacterial groups that utilized the root exudates from $^{13}CO_2$-labeled rice. The transcriptomes of leaf and root and P. aeruginosa and R. erythropolis were performed following a standard protocol. The phoD gene extraction and phoD-harboring microbial community sequencing of rhizosphere soil microbes were performed following a standard protocol. The P-releasing ability of soil bacteria and P accumulation in R. erythropolis were measured by Raman spectroscopy. The surface functional groups of P. aeruginosa were determined by attenuated total reflectance Fourier transform infrared (ATR-FTIR) spectroscopy. All those have been well described in the manuscript. The Al^{3+}, available Al, and other nutrient elements were obtained using inductively coupled plasma–optical emission spectrometry (ICP–OES, PerkinElmer Avio 200, Waltham, MA) and ion chromatography (Dionex ICS-900, USA). Y.L., C.L., M.J., M.Y., Z.M., L.Z., and J.D. contributed experiments and analysis.
Timing and spatial scale	The field experiment was set up at the Yingtan Agroecosystem Field Experiment Station of the Chinese Academy of Sciences (116°55 '30' E, 28°15 '20' N) located in Jiangxi Province, China. The 248 unique microbial strains were isolated from field rice rhizosphere soil samples in 2019. A synthetic community (SynCom) was derived from two efficient Al-resistant strains in the 248 unique strains in 2020. The field experiment data and samples for this study were collected in Oct. 2021. The greenhouse experiments were lasted during Jul. 2020-May. 2022 to explore the growth-promoting effect and growth-promoting mechanisms of the SynCom.
Data exclusions	No data were excluded from the analyses.
Reproducibility	The findings in this paper were remarkably reproducible. For pot experiment, the microbial inoculation experiments was independently performed more than 3 times.
Randomization	The field and plant pot experiments were assigned to different treatment randomly. Soil samples were collected randomly for each condition in all experiments.
Blinding	All the soil sample processing and field measurements were done following the same way without signs/labels noting the relevant treatment.

Did the study involve field work? ☒ Yes ☐ No

Field work, collection and transport

Field conditions	The field experiment was performed at the Yingtan Agrcosystem Field Experiment Station of the Chinese Academy of Sciences. The experimental site has a subtropical monsoon climate with a mean annual temperature of 17.8 °C and precipitation of 1785 mm. The accumulated temperature above 10 °C is 5528 °C , and the frost-free period is 262 days. The typical agricultural soil is Ultisol. The soil pH, organic matter, available nitrogen, available phosphorus, available potassium, exchangeable Al^{3+} were 4.32 mg kg^{-1}, 6277.42 mg kg^{-1}, 100.25 mg kg^{-1}, 55.25 mg kg^{-1}, 265.50 mg kg^{-1}, and 2.77 cmol kg^{-1}, respectively.
Location	The field experiment was set up at the Yingtan Agroecosystem Field Experiment Station of the Chinese Academy of Sciences (116°55 '30'' E, 28°15 '20'' N) located in Jiangxi Province, China.
Access & import/export	The property on which the field experiment was built belongs to the Institute of Soil Science, Chinese Academy of Sciences. All the research activities conducted on site comply to national and local laws and regulations, and rules imposed by the Institute of Soil Science, Chinese Academy of Sciences in terms of ecological conservation and work safety.
Disturbance	Each microplot was fenced by 20-cm ridge. The surface of the mud wall was covered with plastic sheet. Prior to planting, all plots were laid out using 20 cm ridge heights. The ridge of the field was covered with plastic sheet.

Reporting for specific materials, systems and methods

We require information from authors about some types of materials, experimental systems and methods used in many studies. Here, indicate whether each material, system or method listed is relevant to your study. If you are not sure if a list item applies to your research, read the appropriate section before selecting a response.

Materials & experimental systems

n/a	Involved in the study	
☒	☐	Antibodies
☒	☐	Eukaryotic cell lines
☒	☐	Palaeontology and archaeology
☒	☐	Animals and other organisms
☒	☐	Clinical data
☒	☐	Dual use research of concern

Methods

n/a	Involved in the study	
☒	☐	ChIP-seq
☒	☐	Flow cytometry
☒	☐	MRI-based neuroimaging